Supporting Information

Ferroptosis Promotes Photodynamic Therapy: Supramolecular Photosensitizer-Inducer Nanodrug for Enhanced Cancer Treatment

Ting Zhu[1#], Leilei Shi[2#], Chunyang Yu[2], Yabing Dong[3], Feng Qiu[1,4], Lingyue Shen[1], Qiuhui Qian[2], Guoyu Zhou[1*], and Xinyuan Zhu[2*]

1. Department of Oral & Maxillofacial-Head & Neck Oncology, Shanghai Key Laboratory of Stomatology, Cosmetic Laser Center, Ninth People's Hospital, Shanghai Jiao Tong University School of Medicine, Shanghai 200011, China.

2. School of Chemistry and Chemical Engineering, Shanghai Key Laboratory for Molecular Engineering of Chiral Drugs, Shanghai Jiao Tong University, Shanghai 200240, China.

3. Department of Dermatology, Huashan Hospital, Fudan University, Shanghai, China.

4. School of Chemical and Environmental Engineering, Shanghai Institute of Technology, Shanghai 201418, China.

[#]These authors contributed equally to this work.

[*]Corresponding authors: G. Zhou. Email: guoyuzhou@hotmail.com and X. Zhu. E-mail: xyzhu@sjtu.edu.cn

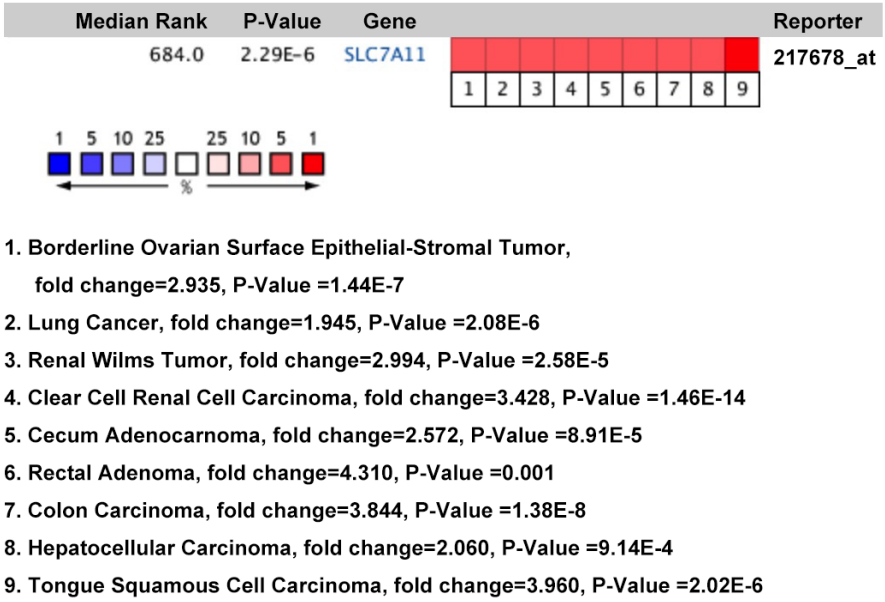

Figure S1. Expression data of 9 different tumors from ONCOMINE database. The colour changes according to a weaker (blue) or higher (red) expression, passing by white, with fluctuating colour intensity. 1. Borderline Ovarian Surface Epithelial-Stromal Tumor[1]. 2. Lung Cancer, not published. 3. Renal Wilms Tumor[2]. 4. Clear Cell Renal Cell Carcinoma[3]. 5. Cecum Adenocarnoma[4]. 6. Rectal Adenoma[5]. 7. Colon Carcinoma[6]. 8. Hepatocellular Carcinoma[7]. 9. Tongue Squamous Cell Carcinoma[8].

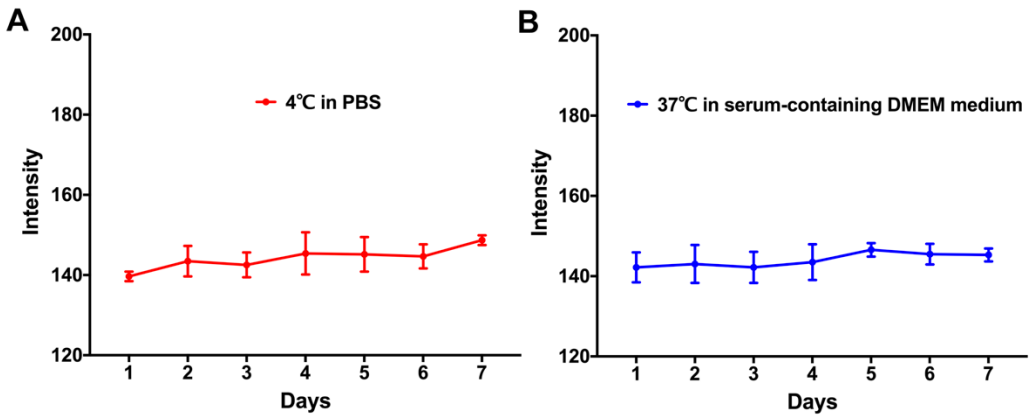

Figure S2. The stability study of Ce6-erastin nanoparticles in different solution.

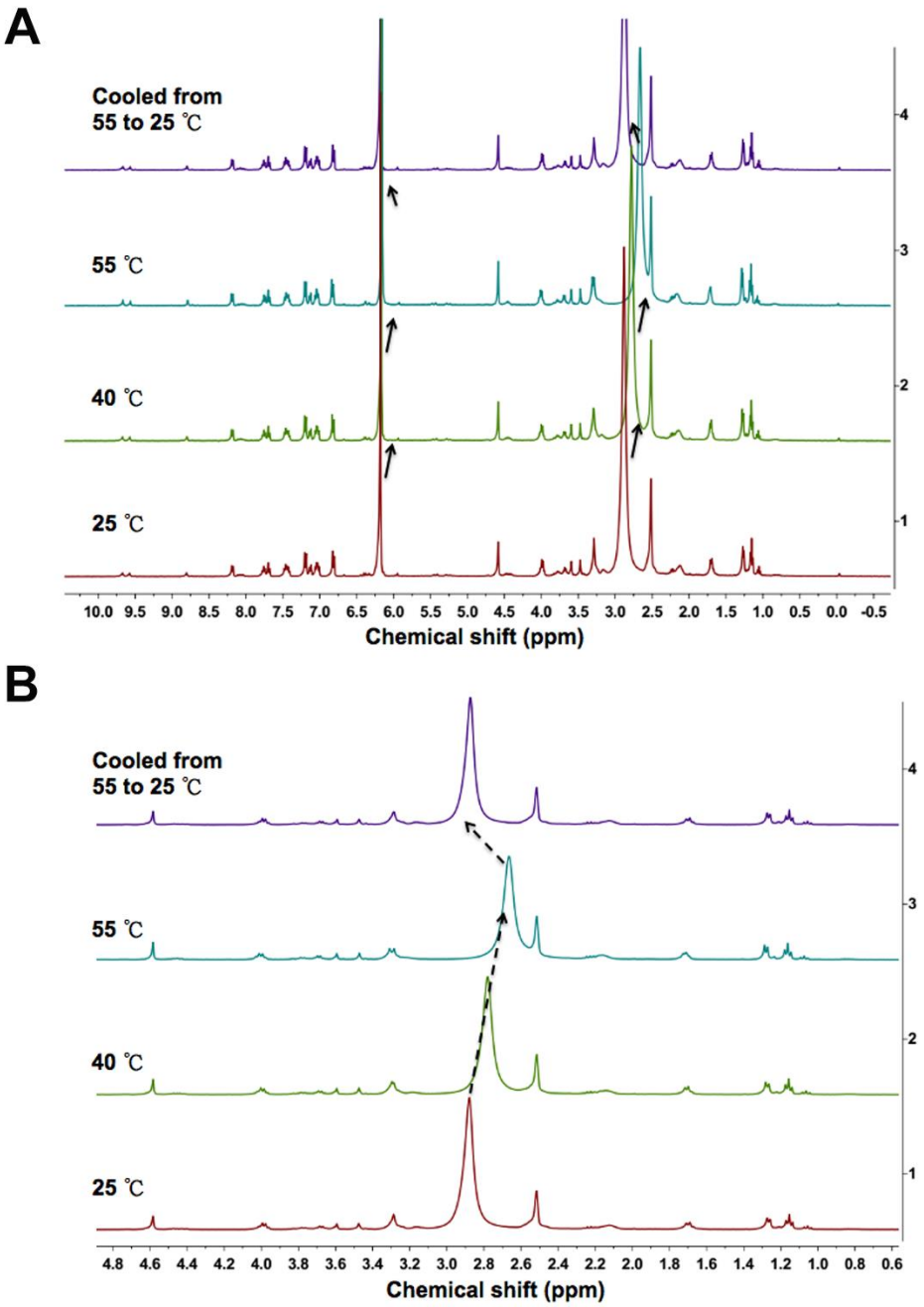

Figure S3. Variable-temperature ^{1}H NMR spectra of the Ce6-erastin nanoparticles. (A) Whole spectra in the region 0-10.0 ppm, (B) magnified spectra in the region 0.6-4.8 ppm. The sample was allowed to equilibrate for 5 min at each temperature. (400 MHz, 1,1,2,2-tetrachloroethane-*d2* : dimethyl sulfoxide-*d6* = 5 : 1).

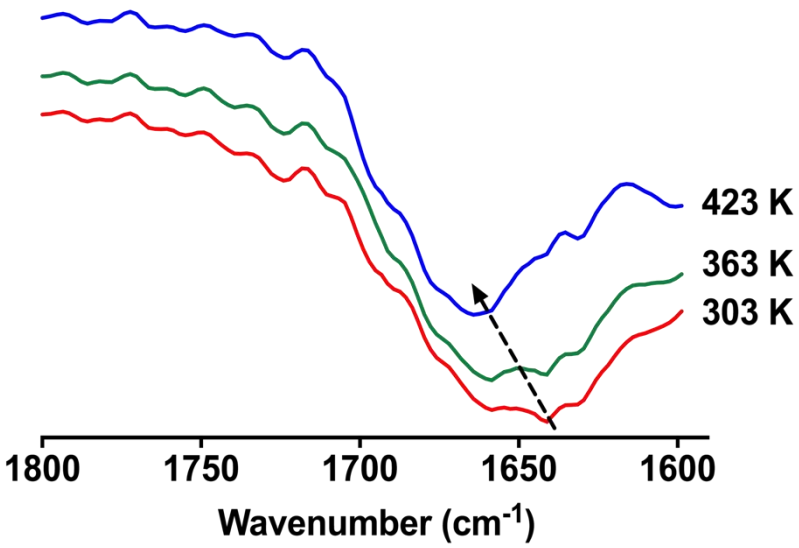

Figure S4. Variable temperature FTIR spectra of Ce6-erastin nanoparticles. Samples were allowed to equilibrate for 10 min at each temperature.

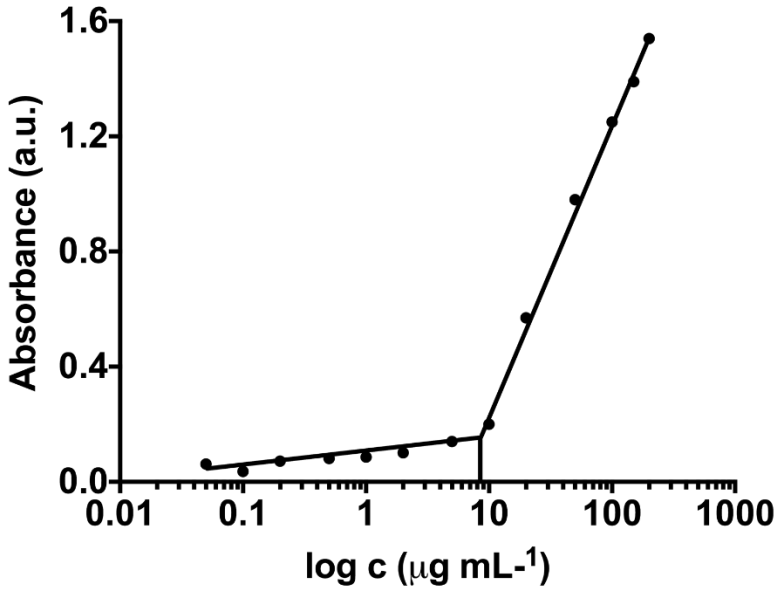

Figure S5. The relationship of UV absorbance of DPH and Ce6-erastin nanoparticles in different concentrations. The CAC value of Ce6-erastin nanoparticles is about 7.94 μg mL^{-1}.

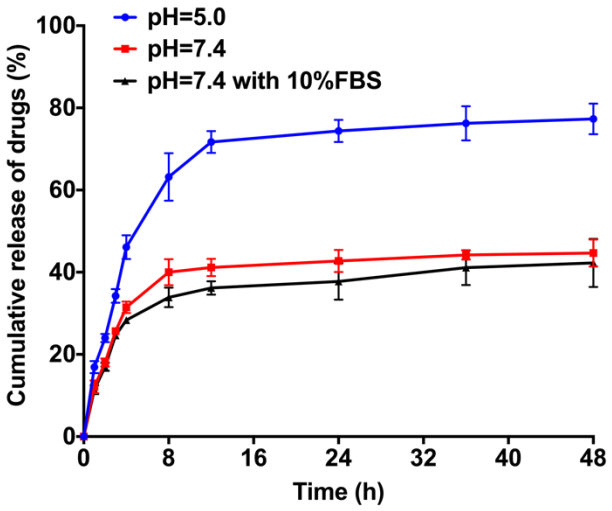

Figure S6. *In vitro* Ce6 release profiles of Ce6-erastin under different conditions (pH = 5.0 and pH =7.4 containing FBS or not).

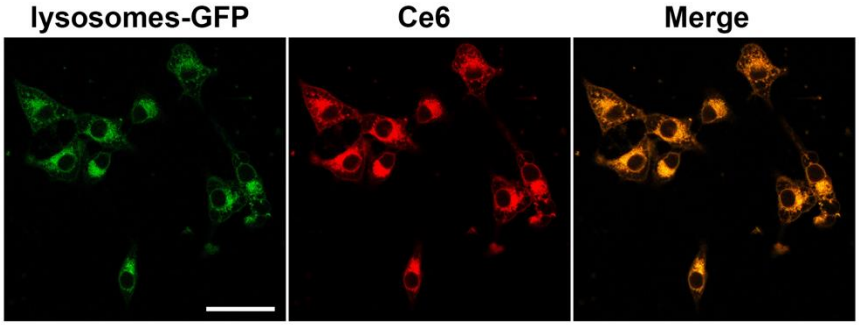

Figure S7. Intracellular distribution of Ce6-erastin in CAL-27 cells at 4 hour incubation, getting from CLSM. Red color shows the intracellular location of Ce6. Green color shows the intracellular location of lysosomes, Scale bar represents 200 μm.

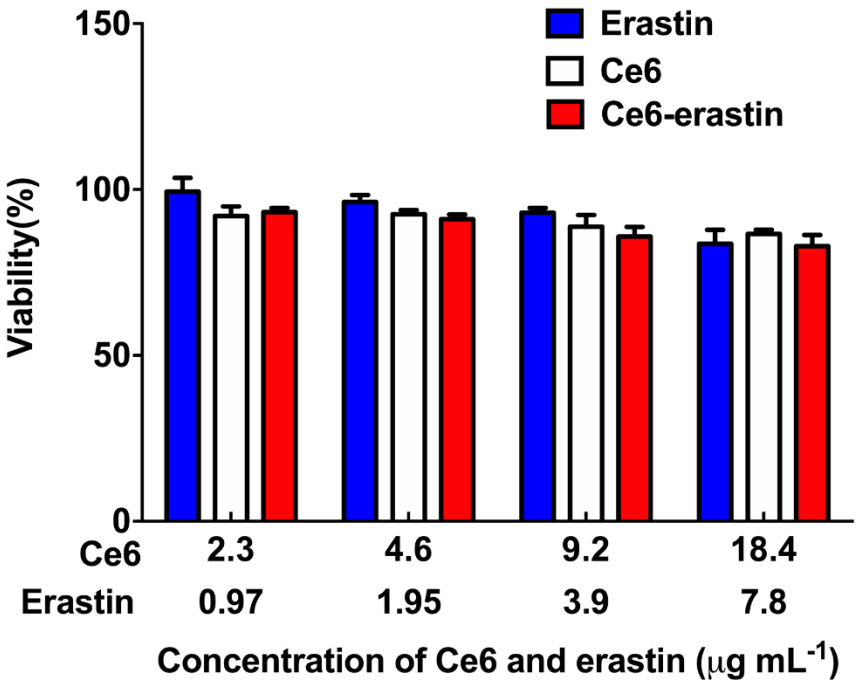

Figure S8. Relative cell viability data of CAL-27 cells treated with erastin, Ce6 and Ce6-erastin nanoparticles in different concentrations 48 hours without laser exposure.

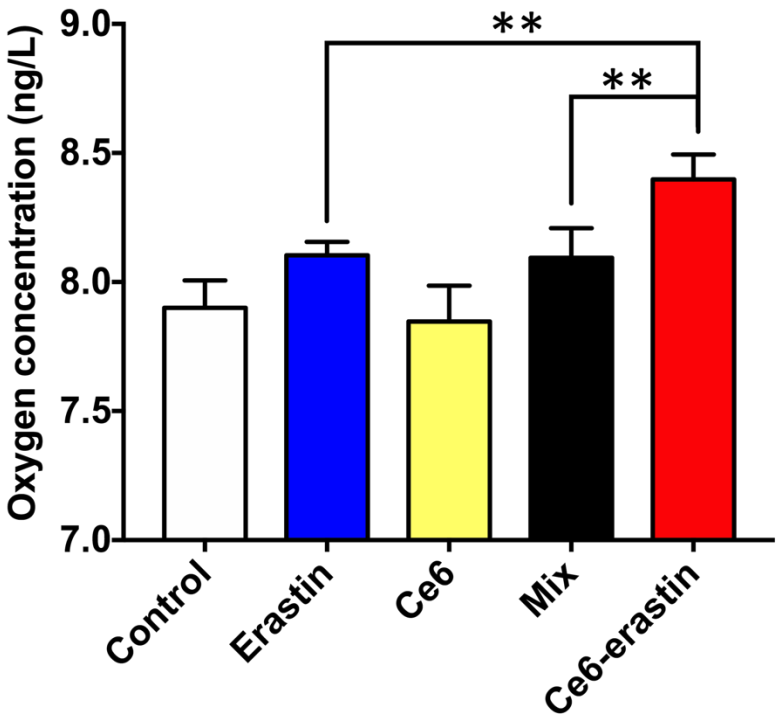

Figure S9. Oxygen concentration of culture medium of CAL-27 cells treated with erastin, Ce6, Ce6/erastin mixture and Ce6-erastin nanoparticles. The statistical significance level is **p*<0.05, ***p*<0.01.

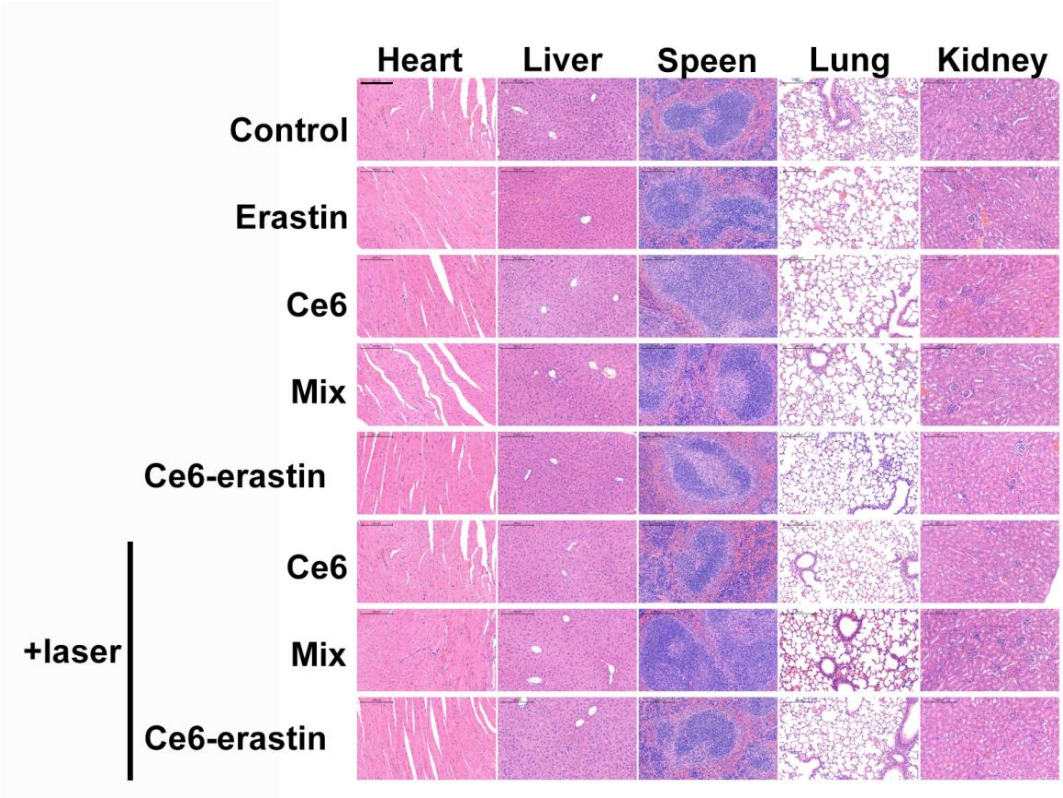

Figure S10. Hematoxylin and eosin (H&E) staining images of livers, spleens, lungs, kidneys and hearts of CAL-27-tumor-xenografted BABL/c nude mice after treating with different formulations. Scales represent 100 μm.

References

1. Anglesio MS, Arnold JM, George J, Tinker AV, Tothill R, Waddell N, et al. Mutation of ERBB2 provides a novel alternative mechanism for the ubiquitous activation of RAS-MAPK in ovarian serous low malignant potential tumors. Mol Cancer Res. 2008; 6: 1678-90.

2. Jones J, Otu H, Spentzos D, Kolia S, Inan M, Beecken WD, et al. Gene signatures of progression and metastasis in renal cell cancer. Clin Cancer Res. 2005; 11: 5730-9.

3. Cutcliffe C, Kersey D, Huang CC, Zeng Y, Walterhouse D, Perlman EJ, et al. Clear cell sarcoma of the kidney: up-regulation of neural markers with activation of the sonic hedgehog and Akt pathways. Clin Cancer Res. 2005; 11: 7986-94.

4. Kaiser S, Park YK, Franklin JL, Halberg RB, Yu M, Jessen WJ, et al. Transcriptional recapitulation and subversion of embryonic colon development by mouse colon tumor models and human colon cancer. Genome Biol. 2007; 8: R131.

5. Sabates-Bellver J, Van der Flier LG, de Palo M, Cattaneo E, Maake C, Rehrauer H, et al. Transcriptome profile of human colorectal adenomas. Mol Cancer Res. 2007; 5: 1263-75.

6. Skrzypczak M, Goryca K, Rubel T, Paziewska A, Mikula M, Jarosz D, et al. Modeling oncogenic signaling in colon tumors by multidirectional analyses of microarray data directed for maximization of analytical reliability. PLoS One. 2010; 5: e13091.

7. Wurmbach E, Chen YB, Khitrov G, Zhang W, Roayaie S, Schwartz M, et al. Genome-wide molecular profiles of HCV-induced dysplasia and hepatocellular carcinoma. Hepatology. 2007; 45: 938-47.

8. Ye H, Yu T, Temam S, Ziober BL, Wang J, Schwartz JL, et al. Transcriptomic dissection of tongue squamous cell carcinoma. BMC Genomics. 2008; 9: 69.